New Journal of Physics
The open access journal at the forefront of physics

Deutsche Physikalische Gesellschaft DPG
IOP Institute of Physics

Published in partnership with: Deutsche Physikalische Gesellschaft and the Institute of Physics

OPEN ACCESS

RECEIVED
6 April 2017

REVISED
19 June 2017

ACCEPTED FOR PUBLICATION
13 July 2017

PUBLISHED
12 October 2017

PAPER

Probing quantum fluctuation theorems in engineered reservoirs

C Elouard[1], N K Bernardes[2], A R R Carvalho[3], M F Santos[4] and A Auffèves[1]

[1] CNRS and Université Grenoble Alpes, Institut Néel, F-38042 Grenoble, France
[2] Departamento de Física, Universidade Federal de Minas Gerais, Belo Horizonte, Caixa Postal 702, 30161-970, Brazil
[3] Centre for Quantum Dynamics, Griffith University, Nathan, Queensland 4111, Australia
[4] Instituto de Física, Universidade Federal do Rio de Janeiro, Caixa Postal 68528, Rio de Janeiro, RJ 21941-972, Brazil

E-mail: alexia.auffeves@neel.cnrs.fr

Keywords: quantum thermodynamics, fluctuation theorems, quantum trajectories

Abstract

Fluctuation theorems (FTs) are central in stochastic thermodynamics, as they allow for quantifying the irreversibility of single trajectories. Although they have been experimentally checked in the classical regime, a practical demonstration in the framework of quantum open systems is still to come. Here we propose a realistic platform to probe FTs in the quantum regime. It is based on an effective two-level system coupled to an engineered reservoir, that enables the detection of the photons emitted and absorbed by the system. When the system is coherently driven, a measurable quantum component in the entropy production is evidenced. We quantify the error due to photon detection inefficiency, and show that the missing information can be efficiently corrected, based solely on the detected events. Our findings provide new insights into how the quantum character of a physical system impacts its thermodynamic evolution.

1. Introduction

The existence of some preferred direction of time is a fundamental concept of physics, captured by the second Law of thermodynamics [1]. The irreversibility of physical phenomena is manifested by a strictly positive entropy production, classically identified with the change of entropy of the closed system considered. In the textbook situation of a system $\mathcal{S}$ exchanging work W with some external operator and heat $Q_{\rm cl}$ with a thermal reservoir $\mathcal{R}$ of temperature T, entropy production equals the sum of the entropy change of the system $\Delta S_{\rm sys}$ and the reservoir $\Delta S_{\rm res} = -Q_{\rm cl}/T$, and reads

$$\Delta_{\rm i} S = (W - \Delta F)/T. \tag{1}$$

ΔF is the change of the system's free energy, satisfying $\Delta S_{\rm sys} = (W + Q_{\rm cl} - \Delta F)/T$.

Focusing on the transformations of microscopic systems, stochastic thermodynamics has extended the concepts of thermodynamics to single stochastic realizations or 'trajectories' of the system in its phase space [2–4]. In this framework, heat and work exchanges become stochastic quantities defined for single trajectories γ, which can give rise to a negative entropy production $\Delta_{\rm i} s[\gamma] < 0$. The fluctuations of $\Delta_{\rm i} s[\gamma]$ verify the central fluctuation theorem (FT) [5] $\langle {\rm e}^{-\Delta_{\rm i} s[\gamma]/k_B} \rangle_\gamma = 1$, where $\langle \cdot \rangle_\gamma$ denotes the average over the trajectories, while the Second Law of thermodynamics remains valid on average. A famous example of such central FT is provided by Jarzynski's equality (JE) [4, 6] characterizing isothermal transformations of systems driven out of equilibrium. Equation (1) remains valid at the trajectory level, such that entropy produced along a single trajectory γ verifies $\Delta_{\rm i} s[\gamma] = (W[\gamma] - \Delta F)/T$. $W[\gamma]$ is the stochastic work exchange for the trajectory γ, yielding JE:

$$\langle {\rm e}^{-W[\gamma]/k_B T} \rangle_\gamma = {\rm e}^{-\Delta F/k_B T}. \tag{2}$$

In the classical regime, the stochastic work exchanges $W[\gamma]$ are inferred from the knowledge of the trajectory, which can be recorded without perturbing the system in principle with an arbitrary precision (figure 1(a)). Using this protocol, JE has been experimentally probed in various setups, e.g. with Brownian particles [7, 8] or electronic systems [9].

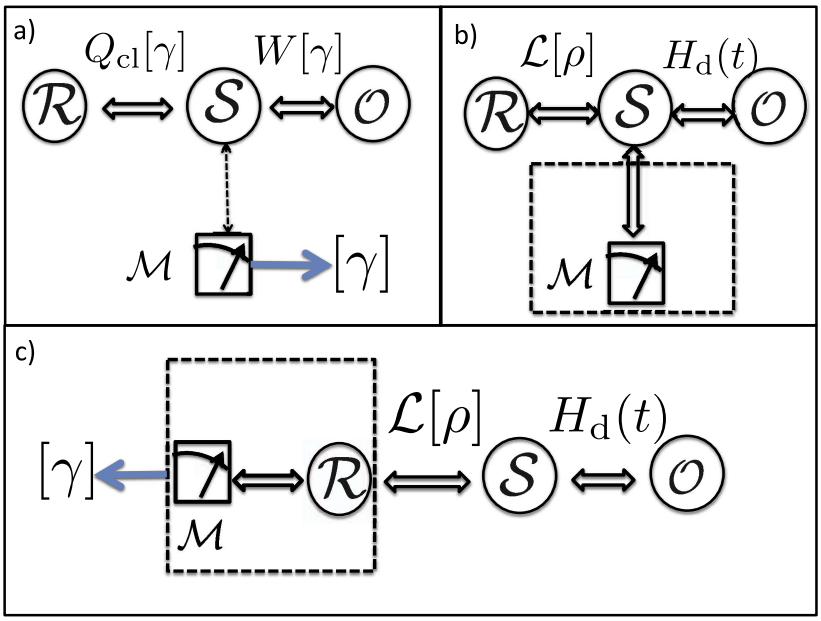

Figure 1. (a) Classical setup to test FT on a system $\mathcal{S}$ exchanging heat with a thermal bath $\mathcal{R}$ and work with an external operator $\mathcal{O}$. The stochastic amounts of heat $Q_{\rm cl}[\gamma]$ and work $W[\gamma]$ are reconstructed by recording the classical trajectory γ of the system. (b) $\mathcal{S}$ is a quantum system driven through a Hamiltonian $H_{\rm d}(t)$ and interacting with a heat bath through the Lindbladian $\mathcal{L}[\rho]$. Monitoring $\mathcal{S}$ can randomly perturb its evolution and corresponds to an additional dissipative channel. (c) Proposed strategy: monitoring a reservoir engineered to simulate a thermal bath.

The recent developments of quantum and nano-technologies have urged to explore the validity of FTs for out-of-equilibrium quantum systems. In the particular case of Jarzynski's protocol, the system coupled to a thermal reservoir can now be coherently driven. However in the quantum world, monitoring a system perturbs its evolution (figure 1(b)), posing severe difficulties to measure and even to define work exchanges. In a series of pioneering papers [10–13] it was shown that JE is still valid and can be probed, provided that the system's (resp. reservoir's) internal energy change $\Delta U[\gamma]$ (resp. $-Q_{\rm cl}[\gamma]$) can be known from projective energy measurements performed at the beginning and at the end of the transformation. The work is then inferred from the First Law: $\Delta U[\gamma] = W[\gamma] + Q_{\rm cl}[\gamma]$. Known as the two-points measurement scheme, this seminal extension of JE in the quantum world has triggered numerous investigations, motivated by two major challenges. The first challenge is practical: How to measure energy changes induced by a microscopic system on a large reservoir? One possible strategy relies on finite size reservoirs whose temperature is sensitive to heat exchanges with the system [14–16], such that both emission and absorption events can be detected using fine calorimetry. But such reservoirs are by essence non Markovian, therefore affecting the dynamics of the system and the resulting work distribution [17].

Another strategy involves the convenient platforms provided by superconducting circuits and semi-conducting quantum photonics. In both cases, the radiation produced by quantum emitters (superconducting qubits or quantum dots) is efficiently funneled into well-designed waveguides, and is thus recorded with high efficiency. This recent experimental ability has lead to the development of bright single photon sources [18, 19] and to the monitoring of quantum trajectories of superconducting quantum bits [20–22]. However, standard schemes based on photo-counters do not allow for the recording of photons absorbed by the system, a major drawback for quantum thermodynamics purposes.

The second challenge is of fundamental nature, and consists in identifying quantum signatures in quantum FTs. For instance, the coupling to a thermal bath erases quantum coherences during the system's evolution. This is an irreversible process, expected to induce some genuinely quantum entropy production [23, 24]. Furthermore, the incoherent energy exchange between the system and the bath (heat) is carried by quantized excitations. Thus any information depending on the recording of these excitations may be significantly hindered by the eventual inefficiency of the detection scheme. So far, an experimental observation of such genuinely quantum effects has remained elusive.

Here we propose a strategy that addresses both the practical and fundamental issues raised above (figures 1(c) and 2). Our proposal is based on an effective two-level system coupled to an engineered thermal bath already introduced by some of us [25, 26] to perform incoherent quantum computing [27]. A great interest of this scheme is that it allows for the detection of the emission and the absorption of photons in the reservoir, while still keeping its Markovian character. Eventually, both the heat exchanges and the quantum trajectory followed by the system can be fully reconstructed. Note that a quite similar strategy is proposed in [28] to access

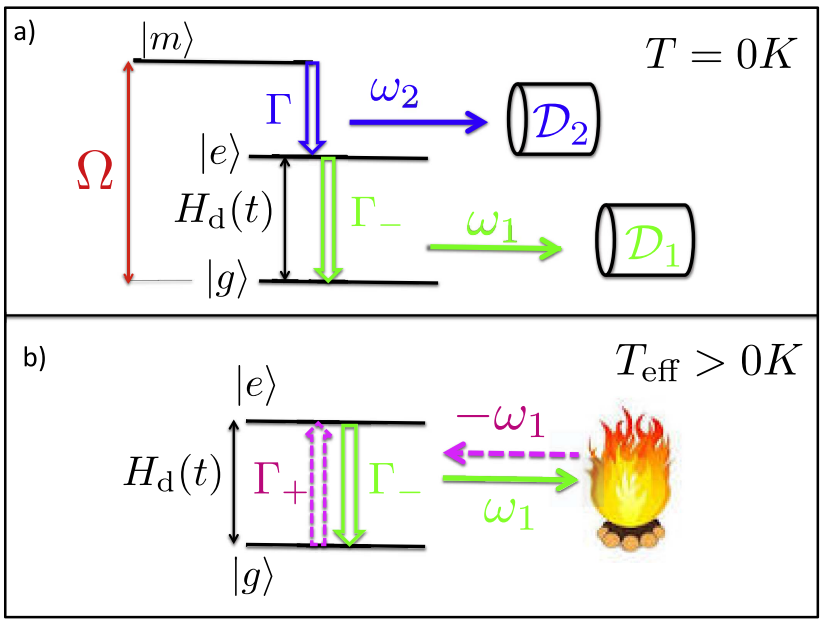

Figure 2. (a) Engineered environment based on a three-level atom. The state $|m\rangle$ has a very short lifetime due to spontaneous emission in vacuum characterized by the rate Γ. The transition $|e\rangle$ to $|g\rangle$ (resp. $|m\rangle$ to $|e\rangle$) is associated with emission of a photon of energy ω_1 (resp. ω_2) detected by $\mathcal{D}_1$ (resp. $\mathcal{D}_2$). The transition $|e\rangle - |g\rangle$ is driven by the Hamiltonian $H_{\rm d}(t)$. (b) Equivalent description in terms of an effective thermal bath. In the presence of a weak classical drive of Rabi frequency Ω resonant with the transition $|m\rangle \rightarrow |e\rangle$, level $|m\rangle$ can be adiabatically eliminated. This result in an effective incoherent rate $\Gamma_+ = 4\Omega^2/\Gamma$ associated with transition $|g\rangle \rightarrow |e\rangle$ (dotted arrow), simulating a qubit coupled to an effective thermal bath of temperature $T_{\rm eff} = \hbar\omega_1/k_B \log(\Gamma_-/\Gamma_+)$.

quantum trajectories of a forced Harmonic oscillator. In the present proposal, the working agent is a qubit, which allows to study the role of coherences between the two energy eigenstates.

We first introduce and validate the platform by checking JE in the simple case where the external drive does not create any coherences in the system, and heat exchanges are perfectly detected. We then turn to the case of a coherence-inducing drive for which we provide a full thermodynamic analysis. Genuinely quantum signatures in thermodynamic quantities are evidenced, as well as how to measure them. Finally, we investigate the influence of the detectors finite efficiency on the expression of the measured FTs. The non-detected heat results in a modified expression of JE that includes an extra term in the entropy production. We show that this term is related to the measurement record and can be computed from the available data.

2. Engineered thermal bath

We consider a system whose three levels are denoted by $|m\rangle$, $|e\rangle$ and $|g\rangle$ of respective energy $E_m > E_e > E_g$ (see figure 2(a)). This three-level system is coupled to an electro-magnetic reservoir at zero temperature, such that $|m\rangle$ decays to state $|e\rangle$ (resp. $|e\rangle$ decays to $|g\rangle$) with a spontaneous emission rate Γ (resp. Γ_-). We assume that $|m\rangle$ is a metastable level, such that $\Gamma \gg \Gamma_-$. We denote $\omega_1 = (E_e - E_g)/\hbar$ and $\omega_2 = (E_m - E_e)/\hbar$. In addition, the atom is weakly driven by a laser resonant with transition $\omega_1 + \omega_2$ and of Rabi frequency Ω, satisfying $\Omega \ll \Gamma$. Due to its short lifetime, level $|m\rangle$ can be adiabatically eliminated, resulting in an effective incoherent transition rate $\Gamma_+ = 4\Omega^2/\Gamma$ from state $|g\rangle$ to state $|e\rangle$ [25]. The states $|e\rangle$ and $|g\rangle$ define our effective qubit of interest (figure 2(b)). Without external drive, this qubit relaxes towards some effective thermal equilibrium characterized by the temperature $T_{\rm eff}$, satisfying $\mathrm{e}^{-\hbar\omega_1/k_B T_{\rm eff}} = \frac{\Gamma_+}{\Gamma_-}$.

In what follows we drive the qubit transition with a Hamiltonian $H_{\rm d}(t)$, such that ω_1 may depend on time: the rates $\Gamma_\pm$ can be adjusted accordingly to keep the effective temperature constant. These adjustments are discussed in [25] and the Methods section at the end of this manuscript. The dynamics of the effective qubit density matrix ρ is ruled by the master equation:

$$\dot{\rho} = -\frac{\mathrm{i}}{\hbar}[H_0 + H_{\rm d}(t),\, \rho] + \Gamma_+\mathcal{L}[\sigma^\dagger]\rho + \Gamma_-\mathcal{L}[\sigma]\rho, \tag{3}$$

where $H_0 = (\hbar\omega_0/2)\sigma_z$ with $\sigma_z = |e\rangle\langle e| - |g\rangle\langle g|$. Note that ω_0 and ω_1 are linked through the relation $\omega_1(t) = \omega_0 + (\langle e|H_{\rm d}(t)|e\rangle - \langle g|H_{\rm d}(t)|g\rangle)/\hbar$. We have introduced the dissipation super-operator $\mathcal{L}[X]\rho = X\rho X^\dagger - \frac{1}{2}\{X^\dagger X,\, \rho\}$, with $\sigma = |g\rangle\langle e|$ and $\{A,\, B\} = AB + BA$. Assuming that a photo-counter $\mathcal{D}_1$ (resp. $\mathcal{D}_2$) detects the photons emitted at frequency ω_1 (resp. ω_2), one can formulate the evolution of the qubit

state conditioned to the measurement records of the detectors in terms of quantum jumps [29]. Assuming an initial known pure state $|\Psi_0\rangle$ of the qubit, and discretizing the time between t_i and t_f such as $t_n = t_\mathrm{i} + n\mathrm{d}t$ (with $n \in [\![0,\, N]\!]$ and $t_N = t_\mathrm{f}$), the evolution of the system features a stochastic trajectory γ of pure states $|\psi_\gamma(t_n)\rangle$. The trajectory is generated by applying a sequence of operators $M_{\mathcal{K}(t_n)}$, where $\mathcal{K}(t_n)$ stands for the stochastic measurement outcome at time t_n.

Namely, detecting a photon on detector $\mathcal{D}_1$ (resp. $\mathcal{D}_2$) at time t_n corresponds to applying the operator $M_1 = \sqrt{\Gamma_-\mathrm{d}t}\,\sigma$ (resp. $M_2 = \sqrt{\Gamma_+\mathrm{d}t}\,\sigma^\dagger$) on the qubit state $|\psi_\gamma(t_n)\rangle$: remarkably in this scheme, the absorption of a photon from the effective heat bath (figure 2(b)) is detectable and actually corresponds to the emission of a photon of frequency ω_2 (figure 2(a)). If no photon is detected, the no-jump operator $M_0 = \mathbb{1} - \mathrm{i}\mathrm{d}tH(t) - \frac{1}{2}M_1^\dagger M_1 - \frac{1}{2}M_2^\dagger M_2$ is applied. Note that this operator induces a non-unitary evolution which captures the update of knowledge ensuing from an absence of detection of photon at time t [30]. The qubit state is then renormalized. Each of these possible evolutions occurs at time t_n with probabilities

$$p_{\mathcal{K}(t_n)} = \langle\psi_\gamma(t_n)|M_{\mathcal{K}(t_n)}^\dagger M_{\mathcal{K}(t_n)}|\psi_\gamma(t_n)\rangle, \quad \mathcal{K} \in \{0,\, 1,\, 2\}. \tag{4}$$

3. Stochastic thermodynamic quantities

We now define the thermodynamic quantities associated with the system's quantum trajectory $|\psi_\gamma(t_n)\rangle$. Following [24], the internal energy of the qubit at time t_n is defined as $U_\gamma(t_n) = \langle\psi_\gamma(t_n)|H(t_n)|\psi_\gamma(t_n)\rangle$, with $H(t) = H_0 + H_\mathrm{d}(t)$ the total Hamiltonian of the system. The variation of this quantity along trajectory γ splits into three terms: there is a work increment $\delta W_\gamma(t_n)$ due to the Hamiltonian time-dependence and given by:

$$\delta W_\gamma(t_n) = \langle\psi_\gamma(t_n)|\mathrm{d}H_\mathrm{d}(t_n)|\psi_\gamma(t_n)\rangle, \quad \mathcal{K}(t_n) = 0. \tag{5}$$

There is also a classical heat $Q_\mathrm{cl}[\gamma]$ corresponding to the energy exchanged with the effective thermal bath under the form of emitted or absorbed excitations of energy $\hbar\omega_1(t_n)$, where $\omega_1(t_n)$ is the qubit effective transition frequency defined as $\omega_1(t) = (\langle e|H(t)|e\rangle - \langle g|H(t)|g\rangle)/\hbar$. This increment reads

$$\delta Q_{\mathrm{cl},\gamma}(t_n) = \begin{cases} -\hbar\omega_1(t_n), & \mathcal{K}(t_n) = 1 \\ \hbar\omega_1(t_n), & \mathcal{K}(t_n) = 2. \end{cases} \tag{6}$$

Finally, a third contribution must be introduced whenever the system's dynamics creates coherences in the $\{|e\rangle;\, |g\rangle\}$ basis. Defined as quantum heat in [24], its increment when a jump takes place reads:

$$\delta Q_{\mathrm{q},\gamma}(t_n) = \begin{cases} \hbar\omega_1(t_n)|\langle g|\psi_\gamma(t_n)\rangle|^2, & \mathcal{K}_\gamma(t_n) = 1 \\ -\hbar\omega_1(t_n)|\langle e|\psi_\gamma(t_n)\rangle|^2, & \mathcal{K}_\gamma(t_n) = 2, \end{cases} \tag{7}$$

while if no jump takes place, it reads

$$\begin{aligned} \delta Q_{\mathrm{q},\gamma}(t_n) = &-\frac{1}{2}\langle\psi_\gamma(t_n)|\{M_1^\dagger M_1 - p_1(t_n),\, H(t_n)\}|\psi_\gamma(t_n)\rangle \\ &- \frac{1}{2}\langle\psi_\gamma(t_n)|\{M_2^\dagger M_2 - p_2(t_n),\, H(t_n)\}|\psi_\gamma(t_n)\rangle, \quad \mathcal{K}_\gamma(t_n) = 0. \end{aligned} \tag{8}$$

The First Law expressed for the trajectory γ is then given by

$$\Delta U[\gamma] = U_\gamma(t_\mathrm{f}) - U_\gamma(t_\mathrm{i}) = W[\gamma] + Q_\mathrm{cl}[\gamma] + Q_\mathrm{q}[\gamma], \tag{9}$$

where $O[\gamma]$ denotes the integrated quantity over the whole trajectory.

4. Jarzynski equality in the quantum regime

Jarzynski's protocol generally consists in preparing the qubit in the thermal equilibrium state $\rho_\mathrm{i} = Z_\mathrm{i}^{-1}\mathrm{e}^{H(t_\mathrm{i})/k_B T_\mathrm{eff}}$, then performing a strong measurement of the qubit energy state to project it on an initial pure state $|i\rangle$ of internal energy U_i. The qubit is driven out of equilibrium until time t_f when a final strong energy measurement is performed, projecting the qubit onto the final state $|f\rangle$ of internal energy U_f. Note that the final density matrix is in general different from the final thermal equilibrium state $Z_\mathrm{f}^{-1}\mathrm{e}^{H(t_\mathrm{f})/k_B T_\mathrm{eff}}$. We have introduced the initial and final partition functions Z_i and Z_f. The two strong measurements allow inferring the qubit internal energy change $\Delta U[\gamma] = U_\mathrm{f} - U_\mathrm{i}$, while the bath monitoring allow recording the classical heat exchange Q_cl. As stated in the introduction (the demonstration is provided in section 5), the entropy produced in a single trajectory γ equals $\Delta_\mathrm{i}s[\gamma] = (\Delta U[\gamma] - Q_\mathrm{cl}[\gamma] - \Delta F)/T_\mathrm{eff}$ [24, 31]. Inserting equation (9), it becomes

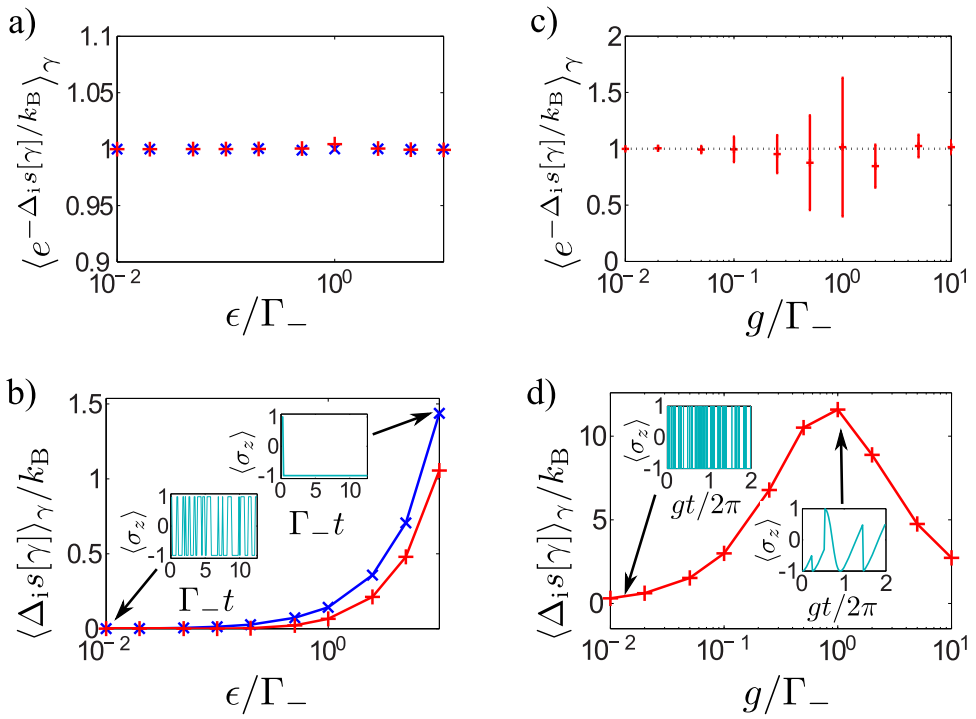

Figure 3. (a), (c) Evolution of the parameter $\langle e^{-\Delta_i s[\gamma]/k_B}\rangle_\gamma$ and (b), (d) of the mean entropy production $\langle \Delta_i s[\gamma]\rangle_\gamma$. We have considered the case of Landauer's drive $H_d(t) = (\hbar\omega_1/2)\,\epsilon\,(t - t_i)\sigma_z$ for (a), (b) and of a coherent drive $H_d(t) = (\hbar g/2)(\sigma e^{i\omega_1 t} + \sigma^\dagger e^{-i\omega_1 t})$ for (c), (d). Both quantities are studied as a function of the respective driving strengths ϵ/Γ_- and g/Γ_-. Insets: evolution of $\langle\sigma_z\rangle = \langle\psi_\gamma(t)|\sigma_z|\psi_\gamma(t)\rangle$ along a single trajectory γ, in two different regimes of the studied transformation. In (b) two different temperatures are used: $\hbar\omega_1/k_B T_{\rm eff} = 0.3$ (red '+') and $\hbar\omega_1/k_B T_{\rm eff} = 3$ (blue 'x'). In (d), $\hbar\omega_1/k_B T_{\rm eff} = 3$. *Parameters*: Number of trajectories $N_{\rm traj} = 10^5$ for (a), (b), $N_{\rm traj} = 2 \times 10^6$ for (c), (d).

$$\Delta_i s[\gamma] = \frac{1}{T_{\rm eff}}(W[\gamma] - \Delta F) + \frac{Q_q[\gamma]}{T_{\rm eff}}. \tag{10}$$

While fully compatible with former expressions for entropy production, equation (10) reveals two components respectively involving the amounts of work and quantum heat exchanged. The second component represents a genuinely quantum contribution due to the presence of quantum coherences in the qubit bare energy basis, that quantitatively relates entropy production and energetic fluctuations. In the following, we show that this quantum contribution can be measured in our setup.

In order to test the platform, we performed numerical simulations using the quantum trajectories method explained at the end of section 2 and implemented using the QuTiP package [32]. The first case considered is the one with driving Hamiltonian $H_d(t) = (\hbar\omega_1/2)\,\epsilon\sigma_z(t - t_i)$ for $t_i \leqslant t \leqslant t_f$. The work and heat exchanged in this case take particularly simple forms, the work being due to time-varying energy levels, and the heat to stochastic population changes induced by the bath. More precisely, we have $\delta W_\gamma(t_n) = \langle\sigma_z(t_n)\rangle\,\hbar\epsilon\,{\rm d}t$ and $\delta Q_{{\rm cl},\gamma}(t_n) = (\langle\sigma_z(t_{n+1})\rangle - \langle\sigma_z(t_n)\rangle)\,\hbar\omega_1(t_n)$, while the quantum heat increment and the quantum component of entropy production are zero. Note that this transformation boils down to the famous Landauer's protocol [8, 33]. In figures 3(a) and (b), we have plotted the quantity $\langle e^{-\Delta_i s[\gamma]/k_B}\rangle_\gamma$ and mean entropy production $\langle\Delta_i s[\gamma]\rangle_\gamma$ for different values of the coupling constant ϵ and temperatures. First note that, as expected, JE is verified for the thermodynamic quantities previously defined. Also note that the entropy production vanishes for $\epsilon \ll \Gamma_-$. This is also expected since, in this limit of weak driving, the transformation is quasi-static and the qubit is always in equilibrium with the heat bath. This situation corresponds to a reversible transformation and, in our example, amounts to a large exchange of photons between the system and the bath before the energy of the system significantly changes. Finally, entropy production drastically increases when $\epsilon \gtrsim \Gamma_-$. In this case, very few photons are exchanged and the system is driven far from equilibrium.

We now turn to a case with no classical counterpart by considering a drive $H_d(t) = (\hbar g/2)\,(\sigma e^{i\omega_1 t} + \sigma^\dagger e^{-i\omega_1 t})$ for $t_i < t < t_f$ and $H_d(t_i) = H_d(t_f) = 0$. This can be implemented by coupling the atom with a classical light field resonant with the transition ω_1. It gives rise to Rabi oscillations, i.e. to the reversible exchange of energy (work) between the qubit and the field under the form of the coherent and periodic emission and absorption of photons at the Rabi frequency g. Note that this scenario deviates from the previous one as, here, work exchanges induce coherences and population changes in the qubit bare energy basis.

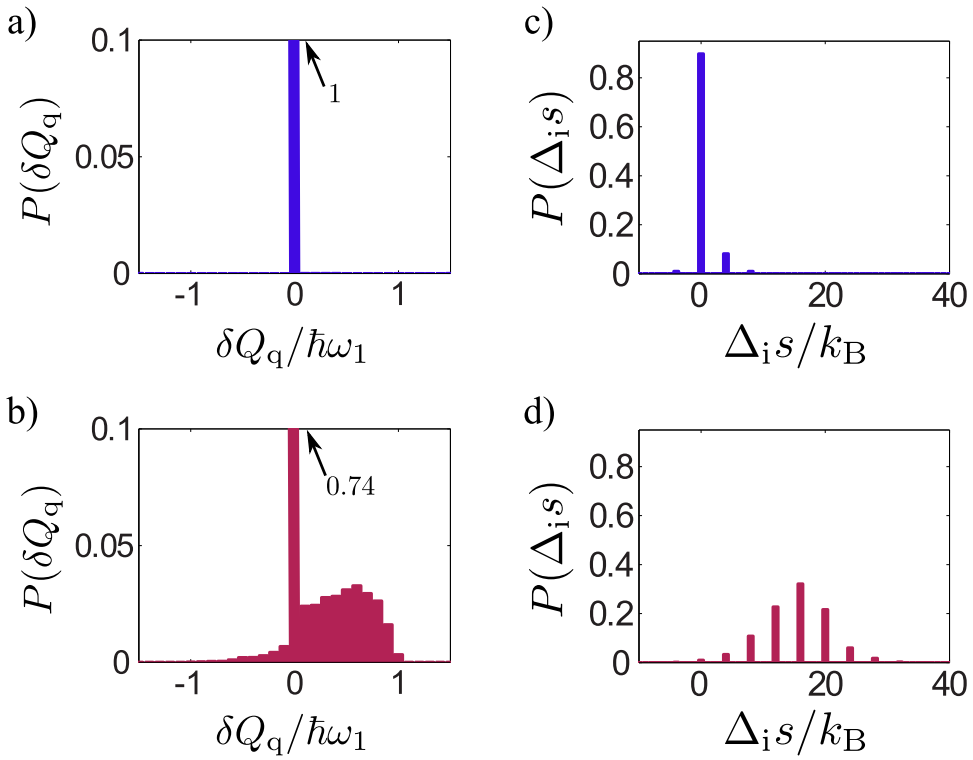

Figure 4. Distributions of the quantum heat increment (a), (b) and of the entropy produced along a single trajectory γ (c), (d) in the case of a coherent drive. *Parameters*: $g/\Gamma_- = 0.01$ (a), (c) and $g/\Gamma_- = 1$ (b), (d). Number of trajectories $N_{\text{traj}} = 10^3$.

According to our definitions, the coupling of this coherently driven qubit to the bath will now give rise to both classical and quantum heat exchanges, as well as a quantum component in the entropy production.

We first check that JE is recovered from the detection events in this quantum regime, as it appears in figure 3(c). This shows that our generalized thermodynamic quantities are properly defined. A more thorough analysis can be drawn from figure 3(d), where we plot the average entropy production as a function of the ratio g/Γ_-. There, one can identify three different situations, two of which corresponding to reversible transformations ($\langle\Delta_i s\rangle_\gamma \to 0$). For a very weak drive $g \ll \Gamma_-$, the qubit is always in a thermal equilibrium state. This regime corresponds to reversible quasi-static isothermal transformations. In the other extreme, i.e. when $g \gg \Gamma_-$, the drive is strong enough to induce almost unperturbed Rabi oscillations. In this case, the transformation is too fast to allow for a stochastic event to take place and heat to be exchanged, i.e. it is adiabatic in the thermodynamic sense and once again reversible.

The intermediate scenario where $g \sim \Gamma_-$ gives rise to a maximal average entropy production. Note that, in this situation, the thermodynamic time arrow has a completely different nature from the classical case studied before. Here, entropy is mostly produced by the frequent interruptions of the qubit Rabi oscillations caused by the stochastic exchanges of photons with the bath (a.k.a. heat) (inset of figure 3(d)). During such quantum jumps, the quantum coherences induced by the driving process are erased, giving rise to the exchange of quantum heat, and to entropy production of quantum nature. The deep connection between quantum heat and entropy production is captured in equation (10) where they are quantitatively related, and in figure 4, where both histograms concentrate around zero in the reversible regime, and take finite values in the irreversible regime. Such a connection between quantum irreversibility and energy fluctuations has already been evidenced in [24] in a different context, where stochasticity is caused by quantum measurement instead of a thermal bath. In both cases, quantum heat exchanges and entropy production appear as two thermodynamic signatures of the same phenomenon, i.e. coherence erasure.

5. Finite detection efficiency

Up to now, we have assumed that the detection of heat is 100% efficient, i.e. that all the photons emitted by the three level atom can be detected. In practice, state-of-the art devices only allow for a fraction η of these photons to be indeed detected [34, 35]. A more realistic scenario is now investigated by considering that the photo-detectors have a finite efficiency η. As a consequence, between two detected photons, there exist several different

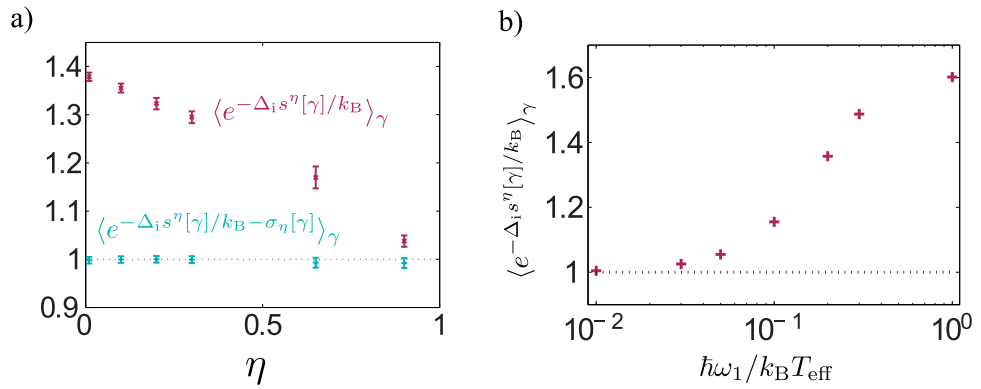

Figure 5. Test of Jarzynski equality at finite efficiency, for a drive $H_d(t) = \hbar\omega_1\epsilon(t - t_i)/2\sigma_z$. (a) Purple 'x': measured parameter $\langle e^{-\Delta_i s^\eta[\gamma]/k_B}\rangle_\gamma$. The magnitude of the deviation (positive for this transformation) increases monotonically when η decreases. Blue '+': the plotted parameter included the correction term $\sigma[\gamma]$. We have used $N_{\rm traj} = 10^4$ trajectories γ and 10^4 ficitious trajectories γ_F for each trajectory. The error bars stand for the standard deviation divided by $\sqrt{N_{\rm traj}}$. (b) Jarzynski's parameter without correction for $\eta = 0.1$ as a function of the temperature. The error bars are smaller than the marker size. *Parameters*: for (a) $\hbar\omega_1/k_BT_{\rm eff} = 0.1$, $\Gamma_- t_f = 0.5$, $\epsilon/\Gamma_- = 600$. For (b): $\Gamma_- t_f = 1$, $\epsilon/\Gamma_- = 9$, $N_{\rm traj} = 10^5$.

possible (or fictitious) trajectories of pure states, which cannot be distinguished by the measurement record: Each of these trajectories corresponds to a particular sequence of undetected emissions and absorptions. This effect induces a decrease of the purity of the qubit state which has to be described by a stochastic density matrix ρ_γ, rather than a wavevector. In the limit where $\eta = 0$ (no detector), the evolution of this density matrix is captured by equation (3), such that $\rho_\gamma(t) = \rho(t)$.

For $0 < \eta < 1$, the evolution of $\rho_\gamma(t)$ is still conditioned on the stochastic measurement outcome of the detector $\mathcal{K}_\gamma(t_n)$, that now corresponds to applying a set of super-operators $\{\mathcal{E}_\mathcal{K}^{(\eta)}[\rho_\gamma]\}$ ($\mathcal{K} \in \{0, 1, 2\}$). Detecting one photon in detector $\mathcal{D}_1$ (resp. $\mathcal{D}_2$) between time t_n and $t_n + dt$ corresponds to applying the super-operator $\mathcal{E}_1^{(\eta)}[\rho_\gamma] = \eta M_1\rho_\gamma M_1^\dagger$ (resp. $\mathcal{E}_2^{(\eta)}[\rho_\gamma] = \eta M_2\rho_\gamma M_2^\dagger$), which occurs with probability $p_1^{(\eta)}(t) = \eta\,\mathrm{Tr}\{M_1^\dagger M_1\rho_\gamma(t)\}$ (resp. $p_2^{(\eta)}(t) = \eta\,\mathrm{Tr}\{M_2^\dagger M_2\rho_\gamma(t)\}$). When no photon is detected, which occurs with probability $p_0^{(\eta)} = 1 - p_1^{(\eta)} - p_2^{(\eta)}$, a super-operator decreasing the state purity is applied:

$$\mathcal{E}_0^{(\eta)}[\rho_\gamma] = \mathbb{1} - \mathrm{i}dt[H(t),\,\rho_\gamma(t)] - \frac{\eta dt}{2}(\Gamma_-\{\sigma^\dagger\sigma,\,\rho_\gamma(t)\} + \Gamma_+\{\sigma\sigma^\dagger,\,\rho_\gamma(t)\}) + (1 - \eta)(\Gamma_- dt\mathcal{L}[\sigma] + \Gamma_+ dt\mathcal{L}[\sigma^\dagger])\rho_\gamma(t). \quad (11)$$

Note that $\mathcal{E}_0^{(\eta)}$ is a linear interpolation between $\mathcal{E}_0^{(1)}[\rho] = M_0\rho_\gamma M_0^\dagger$ applied in the perfect efficiency quantum jump formalism and $\mathcal{E}_0^{(0)}[\rho]$ which is the Lindbladian (right-hand terms in equation (3)). After applying the super-operator $\mathcal{E}_\mathcal{K}^{(\eta)}$, the density matrix has to be divided by $p_\mathcal{K}^{(\eta)}$ in order to be renormalized.

Generalized Jarzynski equality

We now extend the definitions of thermodynamic quantities into the finite efficiency regime. For the sake of simplicity, we restrict the study to a driving Hamiltonian of the form $H_d(t) = (\hbar\omega_1/2)\epsilon(t - t_i)\sigma_z$, such that no quantum heat is exchanged. With the definitions proposed above, the increment of measured classical heat reads:

$$\delta Q_{\rm cl}^\eta(t_n) = \begin{cases} -\hbar\omega_1(t_n), & \mathcal{K}(t_n) = 1 \\ \hbar\omega_1(t_n), & \mathcal{K}(t_n) = 2. \end{cases} \quad (12)$$

Despite its apparent similarity with the definition in the perfect efficiency regime, this energy flow does not capture the entire classical heat flow dissipated in the heat bath, as it does not take into account the energy carried by the undetected photons. One can define the 'measured' entropy production $\Delta_i s^\eta[\gamma] = (\Delta U - Q_{\rm cl}^\eta[\gamma] - \Delta F)/T_{\rm eff}$, i.e. the entropy production computed from the detected photons only. However, this quantity does not check JE as evidenced in figures 5(a) and (b). The violation of JE is all the larger as the efficiency η is smaller, and JE is recovered in the limit $\eta \to 1$, showing that our definitions for the finite-efficiency case still hold in the perfect efficiency limit. Remarkably, however, it is possible to formulate another equality taking into account the finite efficiency, converging towards the standard JE when $\eta \to 1$:

$$\left\langle \mathrm{e}^{-\Delta_{\mathrm{i}} s^{\eta}[\gamma]/k_B - \sigma_\eta[\gamma]} \right\rangle_\gamma = 1. \tag{13}$$

This equality is reminiscent of JE, but it includes a trajectory-dependent correction term $\sigma_\eta[\gamma]$. We now show that $\sigma_\eta[\gamma]$ can be computed from the measurement record only.

The entropy creation along one trajectory γ is usually defined as $\Delta_{\mathrm{i}} s[\gamma] = k_B \log(P_{\mathrm{d}}[\gamma]/P_{\mathrm{r}}[\gamma^{\mathrm{r}}])$, where $P_{\mathrm{d}}[\gamma]$ is the probability of a trajectory γ in the direct protocol defined by $H_{\mathrm{d}}(t)$:

$$P_{\mathrm{d}}[\gamma] = p_{\mathrm{i}} \,\mathrm{Tr}\left\{ |f\rangle\langle f| \left(\overleftarrow{\prod_{n=1}^{N}} \mathcal{E}^{(\eta)}_{\mathcal{K}_\gamma(t_n)} \right) [|i\rangle\langle i|] \right\}. \tag{14}$$

We have introduced $p_{\mathrm{i}} = Z_{\mathrm{i}}^{-1} \mathrm{e}^{-U_{\mathrm{i}}/k_B T_{\mathrm{eff}}}$ the probability of drawing the initial pure state $|i\rangle\langle i|$ of internal energy U_{i} in the initial thermal distribution. The arrow indicates the order in which the sequence of super-operators is applied. $P_{\mathrm{r}}[\gamma^{\mathrm{r}}]$ is the probability of the time-reversed trajectory γ^{r} corresponding to γ. It is generated by the time-reversed drive $H_{\mathrm{d}}(t_{\mathrm{f}} - t)$ and the reversed sequence of super-operators $\mathcal{E}^{(\eta),r}_{\mathcal{K}_\gamma(t_n)}$ [24, 36, 37], such that:

$$P_{\mathrm{r}}[\gamma^{\mathrm{r}}] = p_{\mathrm{f}} \,\mathrm{Tr}\left\{ |i\rangle\langle i| \left(\overleftarrow{\prod_{n=1}^{N}} \mathcal{E}^{(\eta),\mathrm{r}}_{\mathcal{K}_\gamma(t_n)} \right) [|f\rangle\langle f|] \right\}, \tag{15}$$

where $p_{\mathrm{f}} = Z_{\mathrm{f}}^{-1} \mathrm{e}^{-U_{\mathrm{f}}/k_B T_{\mathrm{eff}}}$ the probability of drawing the final pure state $|f\rangle\langle f|$ of internal energy U_{f} in the final thermal distribution.

When $\eta = 1$, the time-reversed operators at time t_n reduce to

$$\mathcal{E}^{(1),\mathrm{r}}_1[\rho_\gamma](t_n) = \mathrm{e}^{-\hbar\omega_1(t_n)/k_B T_{\mathrm{eff}}} M_1^\dagger \rho_\gamma M_1, \tag{16}$$

$$\mathcal{E}^{(1),\mathrm{r}}_2[\rho_\gamma](t_n) = \mathrm{e}^{\hbar\omega_1(t_n)/k_B T_{\mathrm{eff}}} M_2^\dagger \rho_\gamma M_2, \tag{17}$$

$$\mathcal{E}^{(1),\mathrm{r}}_0[\rho_\gamma](t_n) = M_0^\dagger \rho_\gamma M_0. \tag{18}$$

By inserting these expressions in equation (15), we express the ratio $P_{\mathrm{r}}[\gamma^{\mathrm{r}}]/P_{\mathrm{d}}[\gamma] = \mathrm{e}^{-(\Delta U[\gamma] - \Delta F)/k_B T_{\mathrm{eff}}} \, \mathrm{e}^{Q_{\mathrm{cl}}[\gamma]/k_B T_{\mathrm{eff}}}$, which is JE.

When $\eta < 1$, the ratio $P_{\mathrm{r}}[\gamma^{\mathrm{r}}]/P_{\mathrm{d}}[\gamma]$ is modified. It is useful to decompose $\mathcal{E}^{(\eta)}_0$ into three super-operators conserving purity:

$$\mathcal{E}^{(\eta)}_0 = \mathcal{E}^{(\eta)}_{00} + \mathcal{E}^{(\eta)}_{01} + \mathcal{E}^{(\eta)}_{02}, \tag{19}$$

with

$$\begin{aligned} \mathcal{E}^{(\eta)}_{01}[\rho_\gamma] &= (1-\eta)\mathcal{E}^{(1)}_1[\rho_\gamma], \\ \mathcal{E}^{(\eta)}_{02}[\rho_\gamma] &= (1-\eta)\mathcal{E}^{(1)}_2[\rho_\gamma], \\ \mathcal{E}^{(\eta)}_{00}[\rho_\gamma] &= \mathcal{E}^{(1)}_0[\rho_\gamma]. \end{aligned} \tag{20}$$

From this decomposition, we generate a set $\mathcal{F}[\gamma]$ of fictitious trajectories γ_F of pure states, compatible with γ: a trajectory $\gamma_F \in \mathcal{F}[\gamma]$ is built by applying a sequence of super-operators $\{\mathcal{E}_{\mathcal{K}_{\gamma_F}(t_n)}\}_n$, with $\mathcal{K}_{\gamma_F}(t_n) = \mathcal{K}_\gamma(t_n)$ if $\mathcal{K}_\gamma(t_n)$ belongs to $\{1, 2\}$ (i.e. when a photon has been detected), and $\mathcal{K}_{\gamma_F}(t_n) \in \{00, 01, 02\}$ when $\mathcal{K}_\gamma(t_n)$ is zero (no photon detected). $\mathcal{F}[\gamma]$ thus contains $3^{\mathcal{N}_0[\gamma]}$ fictitious trajectories, where $\mathcal{N}_0[\gamma]$ is the number of time-steps during which no photon is detected.

The perfect-efficiency fictitious trajectories are interesting because they can be time-reversed using the rules equations (16)–(18), while their probability distribution checks $P_{\mathrm{d}}[\gamma] = \sum_{\gamma_F \in \mathcal{F}[\gamma]} P_{\mathrm{d}}[\gamma_F]$. Eventually, the following equality is derived:

$$\begin{aligned} \sum_\gamma P_{\mathrm{r}}[\gamma^r] &= 1 \\ &= \sum_\gamma \sum_{\mathcal{F}[\gamma]} P_{\mathrm{r}}[\gamma_F^r] \\ &= \sum_\gamma \sum_{\mathcal{F}[\gamma]} P_{\mathrm{d}}[\gamma_F] \mathrm{e}^{-(\Delta U[\gamma_F] - \Delta F - Q_{\mathrm{cl}}[\gamma_F])/k_B T_{\mathrm{eff}}} \\ &= \sum_\gamma P_{\mathrm{d}}[\gamma] \mathrm{e}^{-(\Delta U[\gamma] - \Delta F - Q^\eta_{\mathrm{d}}[\gamma])/k_B T_{\mathrm{eff}}} \\ &\quad \times \sum_{\mathcal{F}[\gamma]} P_{\mathrm{d}}[\gamma_F|\gamma] \mathrm{e}^{-(Q^\eta_{\mathrm{d}}[\gamma] - Q_{\mathrm{cl}}[\gamma_F])/k_B T_{\mathrm{eff}}}. \end{aligned} \tag{21}$$

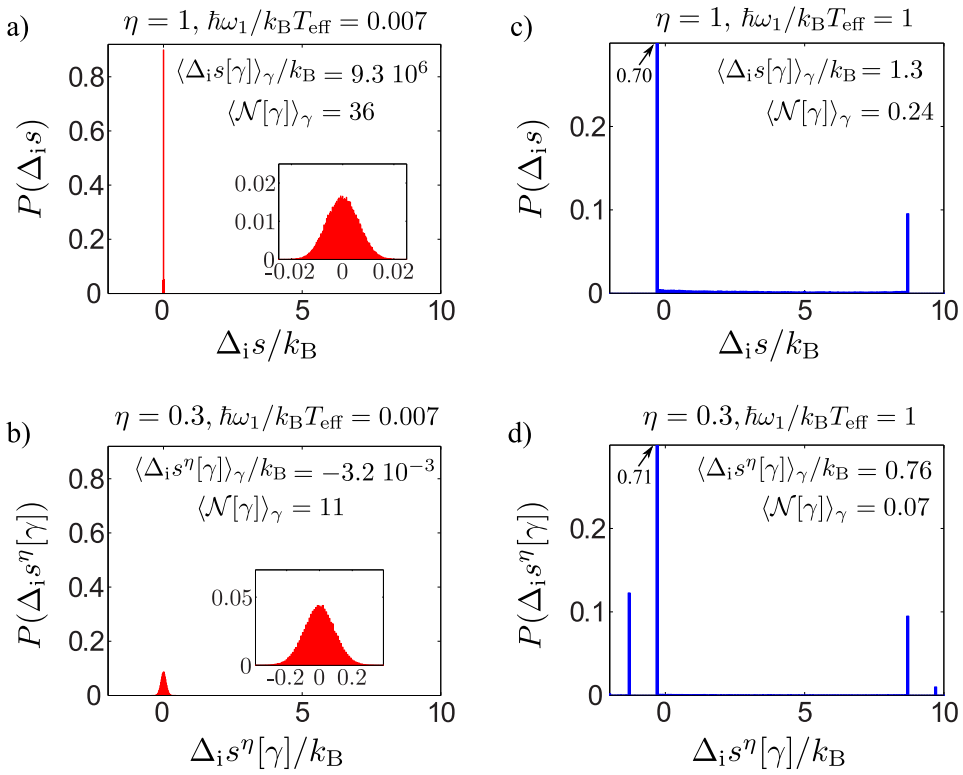

Figure 6. Distributions of the entropy production during the transformation for $\eta = 1$ in (a), (c) and $\eta = 0.3$ in (b), (d). (a) and (b) Correspond to high temperature ($\hbar\omega_1/k_B T_{\rm eff}\,\omega_1 = 7 \times 10^{-3}$) and therefore a large mean number of photons exchanged per trajectory $\langle \mathcal{N}[\gamma]\rangle_\gamma = N - \langle \mathcal{N}_0[\gamma]\rangle_\gamma$. The inserts show the same distribution with rescaled axes to evidence the similarity of shape. (c) and (d) Correspond to a lower temperature ($\hbar\omega_1/k_B T_{\rm eff} = 1$) and a few photon exchanged. *Parameters*: $\Gamma_- t_{\rm f} = 1$, $\epsilon/\Gamma_- = 9$, $N_{\rm traj} = 10^5$.

We have introduced the conditional probability $P_{\rm d}[\gamma_F|\gamma] = P_{\rm d}[\gamma_F]/P_{\rm d}[\gamma]$ of the fictitious trajectory $\gamma_F \in \mathcal{F}[\gamma]$, given the detected trajectory γ. In order to find equation (13), we now define:

$$\sigma_\eta[\gamma] = -\log \sum_{\mathcal{F}[\gamma]} P_{\rm d}(\gamma_F|\gamma)\, {\rm e}^{(Q_{\rm d}[\gamma_F] - Q_{\rm d}^\eta[\gamma])/k_B T_{\rm eff}}. \tag{22}$$

$\sigma_\eta[\gamma]$ can be numerically computed, based solely on the measurement outcomes. The computation involves the simulation of a sample of the trajectories $\gamma_F \in \mathcal{F}[\gamma]$ for each trajectory γ. The corrected expression $\langle {\rm e}^{-\Delta_i s[\gamma]/k_B - \sigma_\eta[\gamma]}\rangle_\gamma$ is plotted in figure 5(a): JE is verified, showing that the experimental demonstration of a FT in a realistic setup is within reach.

Our results explicit a new quantum–classical border in the thermodynamic framework, which is illustrated in figure 6 where the deviation from JE is studied as a function of the reservoir temperature. In the quasi-static limit characterized by $\epsilon \ll \Gamma_-$ (high temperature case), many photons are exchanged and the system is allowed to thermalize before any significant work is done: the transformation is reversible. We see from figures 6(a) and (b) that in this limit, the effect of detection inefficiency in the entropy production is merely to widen the spread of the distribution but conserving its Gaussian shape around zero. The statistical properties of the distribution are not affected, even if many photons are missed, and JE is verified (figure 5(b)). This corresponds to a semi-classical situation where, even though the exchange of heat is quantized, the overall thermodynamic behavior of the system is equivalent to a classical ensemble. In this limit, there is no significant information loss due to the undetected photons.

On the other hand, as soon as work and heat are exchanged at similar rates $\epsilon \sim \Gamma_-$, the system is brought out of equilibrium and the transformation is irreversible. In this limit, few photons are exchanged before a non negligible amount of work is done on the system. Each missed photon represents, then, a significant information loss, such that the measured distribution of entropy production is severely affected (see figures 6(c) and (d)). Such information loss is quantifiable by the violation of the non-corrected JE, and is a direct consequence of the quantization of heat exchanges.

Finally, we emphasize that the derivation of the generalized Jarzynski equality (13) presented in this section is also valid for a drive $H_{\rm d}(t)$ which does not commute with H_0 like the second drive considered in section 4.

6. Conclusion

We presented a realistic setup based on a driven three-level atom allowing to simulate a qubit in equilibrium with an engineered reservoir, giving full access to the distribution of the heat dissipated by the qubit. We exploited this scheme to characterize irreversibility in the case of a coherently driven qubit, coupled to a thermal bath: we evidenced genuinely quantum contributions to the entropy production, and showed these contributions do have some energetic counterpart. In a second part, we took into account finite detection efficiency and evidenced deviations from Jarzynski equality that can be tested and corrected. We derived a modified equality, involving only quantities computed from the finite-efficiency measurement record. This work opens avenues for the experimental verification of FTs in quantum open systems. Owing to the versatility of the scheme, various reservoirs could be simulated, including non-thermal ones. Furthermore, quantitative relations between entropy production and energy fluctuations are the basis for energetic bounds for classical computation [33, 38, 39]. In this work we study situations where equivalent relations can be derived in the quantum regime, providing new tools to explore energetic bounds for quantum information processing.

Acknowledgments

MFS acknowledges CNPq (Project 305384/2015-5). NKB thanks the support from the Brazilian agency CAPES. This work was supported by the Fondation Nanosciences of Grenoble under the Chair of Excellence 'EPOCA', by the ANR under the grant 13-JCJC-INCAL and by the COST network MP1209 'Thermodynamics in the quantum regime'.

Appendix

A.1. Simulating a heat bath with an engineered environment

The rates $\Gamma_\pm$ induce the same dynamics as a heat bath, if and only if

$$\dot{P}_e = -\Gamma_0(2\bar{n}[\omega_1(t)] + 1)\left(P_e(t) - \frac{\bar{n}[\omega_1(t)]}{2\bar{n}[\omega_1(t)] + 1}\right).$$

We have introduced the population of the excited qubit's state $P_e = (\mathrm{Tr}[\rho(t)|e\rangle\langle e|]$, the mean number of thermal photons in the effective bath $\bar{n}[\omega] = (e^{\hbar\omega/k_B T_{\mathrm{eff}}} - 1)^{-1}$ and Γ_0 the spontaneous emission rate of the qubit. The dynamics induced by the engineered environment is:

$$\dot{P}_e = -(\Gamma_+ + \Gamma_-)\left(P_e(t) - \frac{\Gamma_+}{\Gamma_+ + \Gamma_-}\right).$$

By identification, we find the conditions:

$$\Omega(t) = \Gamma_0\sqrt{(\bar{n}[\omega_1(t)] + 1)\bar{n}[\omega_1(t)]}, \tag{23}$$

$$\Gamma_-(t) = \Gamma_0(\bar{n}[\omega_1(t)] + 1). \tag{24}$$

Equation (23) can be fulfilled by tuning accordingly the intensity of the laser drive. Equation (24) requires to tune the incoherent rate of transition from $|e\rangle$ to $|g\rangle$. This task can be performed by embedding the three level atom in a quasi-resonant optical cavity and tuning the frequency between state $|e\rangle$ and $|g\rangle$ e.g. with a non-resonant laser (Stark effect) according to a protocol $\omega_1'(t)$ designed to fulfill equation (24). Note that the implemented protocol $\omega_1'(t)$ is in general different from the target protocol $\omega_1(t)$ which defines the constraints equations (23) and (24) on the qubit dynamics.

A.2. Expression of the quantum heat

For a general driving Hamiltonian $H_d(t) = \delta(t)\sigma_z + \mu(t)\sigma + \mu^*(t)\sigma^\dagger$, the quantum heat $\delta Q_q(t_n)$ exchanged when a jump takes place reads (for $\eta = 1$):

$$\delta Q_q = \begin{cases} \hbar\omega_1(t)P_g(t) - 2\,\mathrm{Re}(\mu(t)\langle\sigma(t)\rangle), & \mathcal{K}_\gamma(t_n) = 1 \\ -\hbar\omega_1(t)P_e(t) - 2\,\mathrm{Re}(\mu(t)\langle\sigma(t)\rangle), & \mathcal{K}_\gamma(t_n) = 2. \end{cases}$$

Between two photon detections, the quantum heat increment reads:

$$\begin{aligned}\delta Q_q(t_n) = &-(\Gamma_- - \Gamma_+)\mathrm{d}t\,\mathrm{Re}(\langle\sigma\rangle)(\hbar\mu(t_n)P_g(t_n) - \hbar\mu^*(t_n)P_e(t_n)) \\ &- \hbar\omega_1(t_n)(\Gamma_- - \Gamma_+)\mathrm{d}tP_e(t_n)P_g(t_n), \quad \mathcal{K}_\gamma(t_n) = 0.\end{aligned} \tag{25}$$

Note that $\delta Q_{\rm q}(t_n)$ is zero when the qubit state has no coherence in $|e\rangle - |g\rangle$ basis, such that $\langle\sigma\rangle = \langle\sigma^\dagger\rangle = 0$, $(P_e(t_n),\ P_g(t_n)) = (1,\ 0)$ (resp. $(0,\ 1)$) when $\mathcal{K}_\gamma(t_n) = 1$ (resp. $\mathcal{K}_\gamma(t_n) = 2$): the qubit has zero probability to absorb a photon at time t when $P_e(t_n) = 1$, and zero probability to emit a photon when $P_g(t_n) = 1$.

References

[1] Lebowitz J 1993 *Phys. Today* **46** 32
[2] Seifert U 2005 *Phys. Rev. Lett.* **95** 040602
[3] Sekimoto K 2010 *Stochastic Energetics* (Berlin: Springer)
[4] Jarzynski C 2011 *Annu. Rev. Condens. Matter Phys.* **2** 329
[5] Seifert U 2008 *Eur. Phys. J.* B **64** 423
[6] Jarzynski C 1997 *Phys. Rev. Lett.* **78** 2690
[7] Toyabe S, Sagawa T, Ueda M, Muneyuki E and Sano M 2010 *Nat. Phys.* **6** 988
[8] Berut A, Arakelyan A, Petrosyan A, Ciliberto S, Dillenschneider R and Lutz E 2012 *Nature* **483** 187
[9] Saira O P, Yoon Y, Tanttu T, Möttönen M, Averin D V and Pekola J P 2012 *Phys. Rev. Lett.* **109** 180601
[10] Talkner P, Lutz E and Hänggi P 2007 *Phys. Rev.* E **75** 050102
[11] Talkner P, Campisi M and Hänggi P 2009 *J. Stat. Mech.* **2** P02025
[12] Esposito M, Harbola U and Mukamel S 2009 *Rev. Mod. Phys.* **81** 1665
[13] Campisi M, Hänggi P and Talkner P 2011 *Rev. Mod. Phys.* **83** 771
[14] Pekola J P, Solinas P, Shnirman A and Averin D V 2013 *New J. Phys.* **15** 115006
[15] Hekking F W J and Pekola J P 2013 *Phys. Rev. Lett.* **111** 093602
[16] Campisi M, Pekola J and Fazio R 2015 *New J. Phys.* **17** 035012
[17] Suomela S, Kutvonen A and Nissila T A 2016 *Phys. Rev.* E **93** 062106
[18] Claudon J, Bleuse J, Malik N S, Bazin M, Jaffrennou P, Gregersen N, Sauvan C, Lalanne P and Gérard J-M 2010 *Nat. Photon.* **4** 174
[19] Somaschi N *et al* 2016 *Nat. Photon.* **10** 340
[20] Ristè D, Dukalski M, Watson C A, de Lange G, Tiggelman M J, Blanter Y, Lehnert K W, Schouten R N and DiCarlo L 2013 *Nature* **502** 350
[21] Murch K W, Weber S J, Macklin C and Siddiqi I 2013 *Nature* **502** 211
[22] Weber S J, Chantasri A, Dressel J, Jordan A N, Murch K W and Siddiqi I 2014 *Nature* **511** 570
[23] Auffèves A 2015 *Physics* **8** 106
[24] Elouard C, Herrera-Martí D A, Clusel M and Auffèves A 2017 *npj Quantum Inf.* **3** 9
[25] Carvalho A R R and Santos M F 2011 *New J. Phys.* **13** 013010
[26] Santos M F and Carvalho A R R 2011 *Europhys. Lett.* **94** 64003
[27] Santos M F, Cunha M T, Chaves R and Carvalho A R R 2012 *Phys. Rev. Lett.* **108** 170501
[28] Horowitz J M 2012 *Phys. Rev.* E **85** 031110
[29] Wiseman H M and Milburn G J 2010 *Quantum Measurement and Control* (Cambridge: Cambridge University Press)
[30] Haroche S and Raimond J M 2013 *Exploring the Quantum: Atoms, Cavities, and Photons* (Oxford: Oxford University Press)
[31] Horowitz J M and Parrondo J M R 2013 *New J. Phys.* **15** 085028
[32] Johansson J R, Nation P D and Nori F 2013 *Comput. Phys. Commun.* **184** 1234
[33] Landauer R 1961 *IBM J. Res. Dev.* **5** 183
[34] Natarajan C M, Tanner M G and Hadfield R H 2012 *Supercond. Sci. Technol.* **25** 063001
[35] Gol'tsman G N, Okunev O, Chulkova G, Lipatov A, Semenov A, Smirnov K, Voronov B, Dzardanov A, Williams C and Sobolewski R 2001 *Appl. Phys. Lett.* **79** 705
[36] Manzano G, Horowitz J M and Parrondo J M R 2015 *Phys. Rev.* E **92** 032129
[37] Crooks G E 2008 *Phys. Rev.* A **77** 034101
[38] Bennett C 1982 *Int. J. Theor. Phys.* **21** 905–40
[39] Faist P, Dupuis F, Oppenheim J and Render R 2015 *Nat. Commun.* **6** 7669